

## Effectiveness of nuchal ligament autograft in the healing of an experimental superficial digital flexor tendon defect in equid

Ahmad Khajeh<sup>1</sup>, Ali Baniadam<sup>1\*</sup>, Ahmad Oryan<sup>2</sup>, Alireza Ghadiri<sup>1</sup>, Hadi Naddaf<sup>1</sup>

<sup>1</sup> Department of Clinical Sciences, Faculty of Veterinary Medicine, Shahid Chamran University of Ahvaz, Ahvaz, Iran; <sup>2</sup> Department of Pathology, School of Veterinary Medicine, Shiraz University, Shiraz, Iran.

### Article Info

#### Article history:

Received: 19 November 2018  
Accepted: 02 February 2019  
Available online: 15 March 2021

#### Keywords:

Equid  
Graft  
Nuchal ligament  
Tendon

### Abstract

This study aimed to investigate nuchal ligament (NL) autograft on experimental tendon defect healing in donkeys. Eight healthy donkeys were used. The left forelimb's superficial digital flexor (SDF) tendon was assigned as treatment, and the right forelimb was allocated as the control group (without surgical intervention). A 3×1.5 cm segment of the funicular part of the NL was excised. A full thickness defect created in the treatment tendon and was grafted with the excised NL. The following parameters were evaluated in 120 days postoperatively: clinical, ultrasonography, radiography, histopathology, biomechanical properties, and scanning and electronic transmission microscopy. There were no significant changes observed in the neck angle so that it was confirmed this treatment regimen preserved the head and neck situation without any considerable neck swelling. Weight-bearing in gait and trot was similar between both forelimbs at the end of the study. Mild to moderate adhesion was detected in the dorsal surface of the SDF tendon. There was no significant difference in the echogenicity and fiber alignment, respectively, on days 90 and 120 after surgery. Treatment significantly amplified the collagen diameter and enhanced the collagen fibril diameter and density considerably compared to the NL. The transplanted tissue was mostly in the remodeling or maturation phase, on day 120 postoperatively. It seems that the NL is biocompatible, almost biodegradable, and effective in tendon healing without metaplasia or tissue rejection.

© 2021 Urmia University. All rights reserved.

### Introduction

Flexor tendon lacerations are frequently associated with significant blunt trauma to the tendon ends, which precludes the tendon's direct apposition and the two ends of the transected tendon taken apart over time is considered as tendon defect.<sup>1</sup> Repair of tendon defect is a more difficult problem than simple repair of a ruptured or lacerated tendon.<sup>1-4</sup> Spontaneous tendon healing results in scar tissue formation that has inferior mechanical properties and disorganized fiber bundles with much higher cellular density than the healthy tissue so that the affected horses are predisposed to high re-injury rates.<sup>5,6</sup>

New treatments for tendon injury focus on the regeneration of functional tissue on cellular and tissue levels.<sup>6</sup> An ideal tendon implant material would have biomechanical properties similar to the normal tendon

and preserve the tendon's gliding function.<sup>1,7</sup> Despite concerns regarding the large size of the harvesting autograft and donor site morbidity, autografts are still the first option in the treatment of tendon defects due to host immune response to allograft and xenograft as well as unavailability of synthetic and biological implants.<sup>2,8,9</sup> Isolating a tendon autograft is usually a difficult task.

The nuchal ligament (NL) is an elastic-collagen structure with elastin dominance on the dorsal midline between the occiput, the cervical vertebrae, and the cranial thoracic that supports the head in an alert position and stretches to accommodate the lowered head in the grazing position.<sup>10-12</sup> The mechanical behavior of NL is the result of the combined properties of its components, including collagen, elastin, glycosaminoglycans, cells, type of alignment, hierarchical organization, and other criteria.<sup>10</sup>

#### \*Correspondence:

Ali Baniadam. DVM, DVSc  
Department of Clinical Sciences, Faculty of Veterinary Medicine, Shahid Chamran University of Ahvaz, Ahvaz, Iran  
E-mail: baniadam@scu.ac.ir



This work is licensed under a Creative Commons Attribution-NonCommercial 4.0 International License which allows users to read, copy, distribute and make derivative works for non-commercial purposes from the material, as long as the author of the original work is cited properly.

The relative similarity of the NL fibers to the flexor tendon components can pose this structure as a scaffold in the healing of this tendon defect. To the best of author's knowledge, there is no available literature regarding the use of NL in the healing of tendon defects. Hence, the present investigation was designed to evaluate the clinical and biomechanical outcomes of healing of the tendon defect, using a NL autograft and assessing the healing quality at the histopathological and ultrastructural level.

## Materials and Methods

**Ethics.** The Animal Care and Research committee of our research center (No. 95-13, 5/30/2016) approved all the current study procedures.

**Animals.** Eight healthy donkeys (age  $5.50 \pm 0.93$  years; weight  $115.25 \pm 15.24$  kg) without abnormalities or lameness based on physical, lameness, and ultrasonography examinations were used in this experiment. Each donkey was kept in a separate box stall a week before surgery and during the first eight weeks of the study while receiving the antiparasitic drug, fed two times per day, and water *ad libitum*. The left forelimb of the animals was assigned as the tendon defect healing group (using NL autograft). The right forelimb was allocated as the control group (without surgical intervention).

**Surgical procedure.** This study was done in two successive stages by the same team. Food and water was withheld 18 and 2 hr before the experiments, respectively. Left jugular vein catheterization of all donkeys was performed using a 14-gauge catheter. In first stage, acepromazine ( $0.05 \text{ mg kg}^{-1}$ , IV; Alfasan, Woerden, The Netherlands) was administered. Twenty minutes later, xylazine ( $0.5 \text{ mg kg}^{-1}$ , IV; Alfasan) and morphine ( $0.1 \text{ mg kg}^{-1}$ , IV; Darou Pakhsh Co., Tehran, Iran) were administered and continued throughout the procedure if needed (one-third of the initial dose to keep the sedation status). The dorsal area of the left funicular part of the NL, between the first two cervical vertebrae and first thoracic vertebra, was anesthetized with a line block using 40.00 mL 1.00% lidocaine hydrochloride (Aburaihan Pharmaceutical Co., Tehran, Iran) in the standing donkey.

A 15.00-cm longitudinal skin incision was made above the cervical vertebrae and just beneath the median fibrous raphe. After retraction of the cervical part of the trapezius muscle and dorsal border of the splenius muscle, the funicular part of the NL was exteriorized. A 3.00 cm in length  $\times$  1.50 cm in width segment was then taken from the ventral area of a funicular part of the NL. The graft was kept in sterile gauze soaked in normal saline. Finally, the muscles and skin were sutured routinely (Fig. 1A). Immediately after the first stage, anesthesia was induced with diazepam ( $0.05 \text{ mg kg}^{-1}$ ; IV, Caspian Tamin Pharmaceutical Co., Rasht, Iran)-ketamine ( $2.20 \text{ mg kg}^{-1}$ , IV;

Alfasan) and maintained with xylazine ( $0.50 \text{ mg kg}^{-1}$ , IV; Alfasan)-ketamine ( $1.10 \text{ mg kg}^{-1}$ , IV). Each donkey was placed in the right lateral recumbency, and the left metacarpal region of the forelimb was prepared for aseptic surgery. A tourniquet was placed above the carpus to minimize the bleeding. A 6.00-cm in length straight skin incision was made in the lateral palmar aspect of the mid metacarpal region (between the accessory carpal bone and proximal sesamoid bone). After the paratenon was exposed and incised, the SDF tendon was separated from the deep digital flexor tendon. A full thickness defect equivalent to two times the tendon width was created using a scalpel blade (Fig. 1B). The autograft extracted from the NL was embedded into the experimental gap. The transected tendon's two stumps were sutured to NL autograft with a double locking-loop suture pattern, using No. 1 polyglycolic acid (PGA; Supa Medical Devices, Tehran, Iran) suture material (Fig. 1C). The NL autograft was covered by paratenon, sutured in a continuous pattern, using the same suture material. The subcutaneous tissue was closed separately using the polyglycolic acid suture material with a simple continuous pattern. Skin closure was accomplished using the nylon suture material in a cruciate suture pattern. The wound was covered with sterile nonadherent gauze. The limb was immobilized using a bandage from the hoof up to proximal to the carpus, followed by application of fiberglass cast from hoof to below the carpal joint.

To support and prevent tearing of the NL autograft in the tendon defect and prevent the pressure on the healing locality and immobilization of the fetlock, casts were applied for eight weeks postoperatively. The casts were changed regularly weekly after day 4 to remove the skin sutures and assess the clinical and ultrasonography parameters. Preoperative and postoperative antibiotic, postoperative analgesic, anti-inflammatory therapy were done as follow: Penicillin-Streptomycin ( $30,000 \text{ IU kg}^{-1}$  penicillin and  $10.00 \text{ mg kg}^{-1}$  streptomycin, IM, Bayer Aflak, Azna, Iran) daily for 5 days, morphine sulfate ( $0.3 \text{ mg kg}^{-1}$ , SC, Darou Pakhsh) twice a day (12 hr apart) for five days, IM administration of 10.00 mL vitamin AD<sub>3</sub>E (Rooyan Darou Pharmaceutical Co., Semnan, Iran), ketoprofen ( $2.00 \text{ mg kg}^{-1}$ ; Razak, Tehran, Iran) for three days after day 3. The donkeys were confined in a stall rest for eight weeks and monitored daily for clinical signs changes. The animals were hand-walked for 20 min daily after the second month and hand-trot for 5 min after the third month postoperatively in addition to hand-walking. To collect the samples, on day 120 after surgery, the donkeys were humanely euthanized, using IV administration of KCl under general anesthesia. Eight specimens belonging to both forelimbs of four donkeys were allocated to biomechanical testing, and the other eight samples were assigned to light and electron microscopic studies.



**Fig. 1.** Two-stage procedure of application of nuchal ligament (NL) autograft in experimental superficial digital flexor tendon defect. **A)** After retraction of the cervical part of the trapezius muscle and dorsal border of the splenius muscle, the funicular part of the NL was exteriorized. A 3.00 cm in length  $\times$  1.50 cm in width segment was then taken from the ventral area of a funicular part of the NL. **B)** Using a surgical blade, a full-thickness defect twice the width of the tendon was created. **C)** The autograft extracted from the NL was embedded into the experimental gap.

**Clinical evaluation.** Clinical index scores including pain in palpation and during flexion of fetlock joint, comfort or discomfort in physical activities, graft survival/rejection by hand-controlled loading (extension and flexion) of the operated limbs with graft manipulation at the grafted SDFT site, tissue reaction, neck swelling, neck deviation, and neck angle; probable head dropping related to the surgical harvest of NL autograft of the treated SDFT were assessed for each donkey before surgery and on days 14, 28, 42, 60, 90 and 120 post-operatively.<sup>7,13</sup> The neck angle was measured between the poll, withers, and vertical projection of a reference marker perpendicular to the ground.<sup>10</sup> Also, the limb circumference at the repair site and proximal and distal to it, height of the fetlock joint to the surface of the ground, and fetlock joint angle were measured using a measuring tape compared to the times as mentioned earlier and with the nonsurgical limb. The fetlock joint angle was measured in donkeys' standing position, using an orthopedic goniometer that calculated the angle from the midcarpal passing through the fetlock joint and ended by the hoof quarter.<sup>14</sup> After cast removal, all donkeys were examined for lameness with two different indices on days 60, 90, and 120 post-operatively.

**Radiography and ultrasonography.** Radiography and ultrasonography were performed for both forelimbs and evaluated by an expert radiologist. Ultrasonographic examinations of SDFT were accomplished just before the surgical intervention and on days 14, 28, 42, 60, 90, and 120 postoperatively with a 7.50 MHz linear transducer (Phoenix Contact, Milton, Canada). The palmar metacarpal region was divided into three portions, A, B, and C. The B portion was defined as the area of transplantation that was nearly 4.00 cm in length. The A and C regions were almost 4 cm in length, just proximal and distal to the transplantation site, respectively. Longitudinal and transverse scans were obtained to assess the tendon echogenicity, alignment of collagen fibers, cross-sectional area (CSA), thickness, and width of SDFT as the healing indicators, compared to the contralateral limb. The tendon echogenicity and alignment of collagen fibers were scored.<sup>2</sup>

The CSA, thickness, and width of SDFT was measured in the transverse section. Radiography from the carpal joint, metacarpal (MC) region, fetlock joint, and the proximal interphalangeal joint was performed in standard views on days 0, 60, 90, and 120 after surgery. The radiographs were interpreted for any bone and soft tissue changes, such as osteoarthritis, bone fracture, tendon calcification, and soft tissue swelling.

**Gross appearance.** The palmar surface of both left and right forelimbs, between the carpal and fetlock joints, were dissected to expose the superficial digital flexor tendon. The overall appearance and characteristics of the repaired tissue regarding peritendinous adhesions, and longitudinal and transverse diameter of the repair site from both ends of tenorrhaphy were grossly evaluated.

**Biomechanical testing.** Biomechanical testing was done according to the method of Dowling *et al.*<sup>16</sup> Briefly; the grafted tendons were harvested by proximal and distal transverse incisions approximately 5.00 cm away from the repair site and a similar location of the contralateral limb. Both the injured and contralateral intact SDFTs were carefully dissected out of the surrounding tissues. The SDFT was cut as much as 4 centimeters proximally and distally to the repair site. All samples were wrapped into sterile moisturized gauze soaked in normal saline and stored at  $-20.00$  °C until tensile testing. Before testing, the tendons were removed from the freezer, thawed for one hour at room temperature. The samples were mounted between two metal clamps with sandpaper inside them to avoid slipping the tendon specimens. The biomechanical test was performed using Santam tensile testing machine (Santam Co., Tehran, Iran) with a 50,000 N load cell. Each tendon was loaded by elongating it at a displacement rate of 6.67 mm per sec until failure. The maximum load (N), yield load (N), stiffness ( $N\ mm^{-1}$ ), ultimate strain (%), yield strain (%), maximum stress ( $N\ mm^{-2}$ ), and modulus of elasticity ( $N\ mm^{-2}$ ) of the samples were extracted from the load-deformation and stress-strain curves.

**Histopathology.** After routine preparation of the samples, they were stained by Hematoxylin and Eosin and

examined under a light microscope (Olympus, Tokyo, Japan).<sup>16</sup> Masson's trichrome staining was used to discriminate collagen fibers, and Verhoeff's iron hematoxylin was applied as specific staining for elastic fiber differentiation on histological sections. The microphotographs were recorded by a digital camera (T-700; Sony Corp., San Diego, USA.) and transferred to Adobe Photoshop software (CS5; Adobe Co., San Jose, USA) for digital analysis.<sup>2</sup>

**Scanning electron microscopy (SEM).** After collecting, the samples, including normal SDFT, normal NL, and grafted tendon, were fixed in cold 4.00% glutaraldehyde. They were then dehydrated with hexamethyldisilazane (TAAB Co., London, UK) and coated initially with osmium tetroxide. Ultimately, they were mounted on copper plates, vacuum-coated with gold, and examined with an SEM (TESCAN-Vega 3.0; Tescan, Brno, Czech Republic), at magnifications from 50× to 50,000×, to identify maturation, differentiation, density, and alignment of collagen fibers in longitudinal and transverse sections.

**Transmission electron microscopy (TEM).** The samples were fixed in 4.00% glutaraldehyde, dehydrated, using a graded series of ethanol dilutions, and embedded in Epon resin (TAAB Co.). The fixed samples were sectioned micro-metrically to evaluate the desired area and then sectioned at 50.00 nm. The nano-metric sections were mounted on microgrids and stained with lead citrate and uranyl acetate. The grids were examined in a TEM (CM 10 transmission electron microscope; Phillips, Eindhoven, The Netherlands).<sup>4</sup> Magnifications of 5000× to 15,000× were used to generate the TEM images. The ultra-micrographs were analyzed using ImageJ software by computerized morphometry (National Institute of Mental Health, Bethesda, USA). The diameter of collagen fibrils of three different fields of the same magnification for each tissue section was measured. For the fibrillar density, ten pictures were captured from 10 horizontal and vertical fields. : The number of collagen fibrils and their diameters in each tissue section's in three different fields were measured. The collagen fibrils were divided, according to their diameter, into four categories 30.00 - 70.00 nm, 70.00 - 130 nm, 130 - 250 nm, and 250 - 360 nm. Also, numbers of the elastic fibers in each field were counted.<sup>4,16</sup>

**Statistical Analysis.** All analyses were performed using SPSS (version 22.0; IBM Corp., Armonk, USA). A paired-samples *t*-test and Wilcoxon signed-rank test were used to analyze the parametric and non-parametric data, respectively, with the confidence level of 95.00%. Results were reported as mean ± standard deviation.

## Results

**Clinical assessment.** All donkeys were calm in a well-padding cast for eight weeks except one donkey that necessitated more cast change due to skin cast sore.

Ultimately the skin soreness improved within ten days after cast removal. Due to unknown causes, one donkey died on day 50, and his tendon specimens were considered for histopathology and ultrastructure evaluations. Weight-bearing in gait and trot was similar between the affected and unaffected forelimbs at the end of four months.

Lameness scores on day 60 were significantly different 2(1-2) compared to the base time and other time points, while on days 90 and 120 showed no significant differences 0(0-2) compared to the base day and were comparable together (AAEP, American Association of Equine Practitioners, lameness scale). Averagely, just on day 14, the animals seemed significantly discomfort relative to the base time, and no tissue rejection was seen. Comparison of pain index at the specific times showed only significant pain reflex on the 14 days 1(1-3) compared to other times. On days 14, 28, 42, and 60, the tissue demonstrated significant reaction compared to the base time. Also, no significant changes were observed in the neck angle, so that it was confirmed that this treatment regimen preserved the head and neck situation without any considerable neck swelling (Table 1).

**Gross appearance.** On 120 post-injury, the NL scaffold was mostly absorbed and substituted by the newly regenerated tendon. The neotendon tissue was homogenous with the original tendon in dorsal and palmar surfaces with the least demarcation between the injured tendon ends and the NL transplant autograft, except for the raised thickening of the tenorrhaphy range site. Mild to moderate adhesion was detected in the superficial digital flexor tendon's dorsal surface, without any adhesion in the palmar surface. There was no evidence of significant residual inflammation, swelling, infection, hyperemia, hemorrhage, necrosis in the treated tendon. New collagen bundles were identified in the longitudinal section of the tendon. Height and transverse diameters of injured treated tendon were significantly higher than the intact tendon (15.50 ± 0.42 versus 10.00 ± 0.25 mm in transverse diameter,  $p = 0.001$ , 3.50 ± 0.11 versus 2.80 ± 0.07 mm in height diameter,  $p = 0.04$ ).

**Radiology and ultrasonography.** Soft tissue swelling was seen on days 60 and 90 after surgery in the treated forelimbs in five donkeys. Except for one donkey, the MC II showed a fractured healing process in the one-third proximal part of the bone. There were no abnormal radiographic signs in the carpal joint, metacarpal bones, fetlock joint, and proximal interphalangeal joint on day 120 postoperatively.

No significant changes were observed in the echogenicity and fiber alignment in the A and C regions of the injured treated tendon, compared to a day before surgery and the contralateral intact tendon on the postoperative days. However, there was a significant increasing trend in the echogenicity and fiber alignment in the B area compared to a day before surgery and the intact contralateral tendon.

**Table 1.** Quantitative results of clinical index owing to the injured treated tendon compared with contralateral intact tendon and neck angle on day 120 post-injury. Data are presented as Mean  $\pm$  SD.

Index	Control	Day 0	Day 14	Day 28	Day 42	Day 60	Day 90	Day 120
Fetlock angle	126.00 $\pm$ 1.31	126.00 $\pm$ 0.54	120.13 $\pm$ 2.03*	119.88 $\pm$ 2.53*	121.00 $\pm$ 1.77*	123.63 $\pm$ 0.92*	125.00 $\pm$ 1.63	125.00 $\pm$ 1.41
Fetlock height	9.31 $\pm$ 0.59	9.28 $\pm$ 0.88	8.50 $\pm$ 0.80*	8.43 $\pm$ 0.62*	8.56 $\pm$ 0.56*	9.12 $\pm$ 0.74	9.29 $\pm$ 0.49	9.29 $\pm$ 0.49
Limb circumference A	13.56 $\pm$ 0.62	13.57 $\pm$ 0.76	13.94 $\pm$ 0.56*	14.00 $\pm$ 0.53*	13.94 $\pm$ 0.62*	13.94 $\pm$ 0.62*	14.00 $\pm$ 0.71*	13.86 $\pm$ 0.69
Limb circumference B	13.56 $\pm$ 0.73	13.57 $\pm$ 0.41	14.12 $\pm$ 0.69	14.12 $\pm$ 0.69	14.19 $\pm$ 0.75*	14.12 $\pm$ 0.92	14.14 $\pm$ 0.85	14.33 $\pm$ 0.83*
Limb circumference C	14.12 $\pm$ 0.64	14.10 $\pm$ 0.51	14.69 $\pm$ 0.62*	14.56 $\pm$ 0.68	14.56 $\pm$ 0.56*	14.56 $\pm$ 0.56*	14.57 $\pm$ 0.73	14.62 $\pm$ 0.69*
Neck angle	51.45 $\pm$ 0.74	51.75 $\pm$ 1.03	51.88 $\pm$ 0.99	52.63 $\pm$ 1.06	51.69 $\pm$ 1.06	51.38 $\pm$ 0.91	51.86 $\pm$ 1.06	50.14 $\pm$ 0.90

\*Asterisk indicates a significant difference compared to base time values ( $p < 0.05$ ).

There was no significant difference in the echogenicity 0(0-1) and fiber alignment 1(0-1), respectively, on days 90 and 120 days after surgery. The lowest echogenicity 3(2-3) was seen on day 14, and the lowest fiber alignment 3(2-3) was seen on days 14 and 28 post-injury.

The significantly increased cross-sectional area was observed from day 42 to 120 in the B and C areas compared to a day before surgery. The B and C cross sections area on day 120 after surgery was 1.58 and 1.35 times greater than before surgery, respectively. The cross-sectional area of the tendon in area A did not increase significantly on day 14 compared to the day before surgery, but gradually the cross-sectional area increased so that on day 120 after surgery, the cross-sectional area of the tendon in area A was 1.45 times larger than before surgery. The significantly increased cross-sectional area was seen in the A and C regions, from day 28 to 120 and day 42 to 120, respectively, compared to the contralateral healthy tendon. In the transplantation site (B area), the increased cross-section was significant from day 14.

**Biomechanical results.** Although treatment with the NL autograft significantly increased the maximum load (N) and yield load (N) compared to those of the intact tendon on day 120 post-injury ( $p = 0.035$  and  $p = 0.009$ , respectively), however, the maximum stress was significantly lower due to the increased cross-sectional area ( $p = 0.016$ ). There were no significant differences in the stiffness, strain, and modulus of elasticity between the treated tendon and the healthy tendon groups (Table 2). The grafted tendon's yield load was significantly higher than that of the intact tendon on day 120 post-injury ( $p = 0.040$ ).

**Histopathological findings.** Micrographs of intact NL stained by Verhoeff's iron Hematoxylin and Masson's trichrome revealed that elastic and collagen fibers were the principal components in which the elastic fibers were dominant (Fig. 2). These fibers were matured, crimped, aligned, and organized unidirectionally. The tissue was

highly cellular with dominant matured fibrocytes aligned parallel to collagen and elastic fibers, and the cellularity of the NL was more than the matured tendon. Significantly few blood vessels were present in the tissue sections of the NL.

Tendon healing in the injured treated tendon belonging to the donkey that died on day 50 post-operatively was in the proliferative or fibroplasia stage. The tissue was highly cellular, mostly irregular, and demonstrated numerous blood vessels (Figs. 2G and 2I). The mesenchymal cells were mostly tenoblasts, and fewer tenoblasts were also present in tissue sections. Fifty days after surgery, the lymphocyte plasma cell, and macrophage counts were still substantially high. The transplanted tissue was mostly in the remodeling or maturation phase, on day 120 post-injury, so that the number of tenoblasts was reduced and the tenocytes count was increased compared to the sample on day 50 postoperatively. The tissue was more aligned, and the number of blood vessels was decreased. However, their diameters were increased. A few lymphocytes and macrophages were seen among the tenocytes and tenoblasts at this stage. Overall, the autograft was seen in three states during the current experiment as follow. Overall, the autograft was seen in three states during the current experiment: 1) Mostly, the transplanted tissue was degraded replaced with the newly formed tendon. 2) The transplanted tissue was degraded, but its remnants were observable. Also, cellularity was reduced, and the graft cells were pyknosed, karyorrhexed, and karyolysed. Also, no cells were seen in some parts. 3) The graft was encapsulated and observed as a part of the primary tissue. Hence, blood flow was maintained, and the NL graft cells remained without any changes.

**Scanning electron microscopy.** The scanning ultra-micrographs illustrated the tendon tissue formation's hierarchy progression in the elastic and collagen fibers bed of the NL autograft. Injured treated tendons with NL

**Table 2.** Biomechanical properties of the tendon samples. Data are presented as Mean  $\pm$  SD.

Variable	L (n = 4)	R (n = 4)	p-Value
Maximum load (N)	1207.60 $\pm$ 254.77	993.87 $\pm$ 198.85	0.035
Yield load (N)	1099.45 $\pm$ 222.32	808.12 $\pm$ 139.67	0.009
Stiffness (N mm <sup>-1</sup> )	162.11 $\pm$ 22.65	179.53 $\pm$ 70.40	0.559
Strain (%)	20.39 $\pm$ 2.74	19.65 $\pm$ 3.18	0.306
Yield strain (%)	16.43 $\pm$ 2.42	13.72 $\pm$ 3.63	0.040
Cross-sectional area (mm <sup>2</sup> )	45.98 $\pm$ 4.97	27.24 $\pm$ 2.04	0.001
Maximum stress (N mm <sup>-2</sup> )	26.05 $\pm$ 3.21	36.31 $\pm$ 5.50	0.016
Modulus of elasticity (N mm <sup>-2</sup> )	148.83 $\pm$ 40.10	232.62 $\pm$ 95.49	0.064



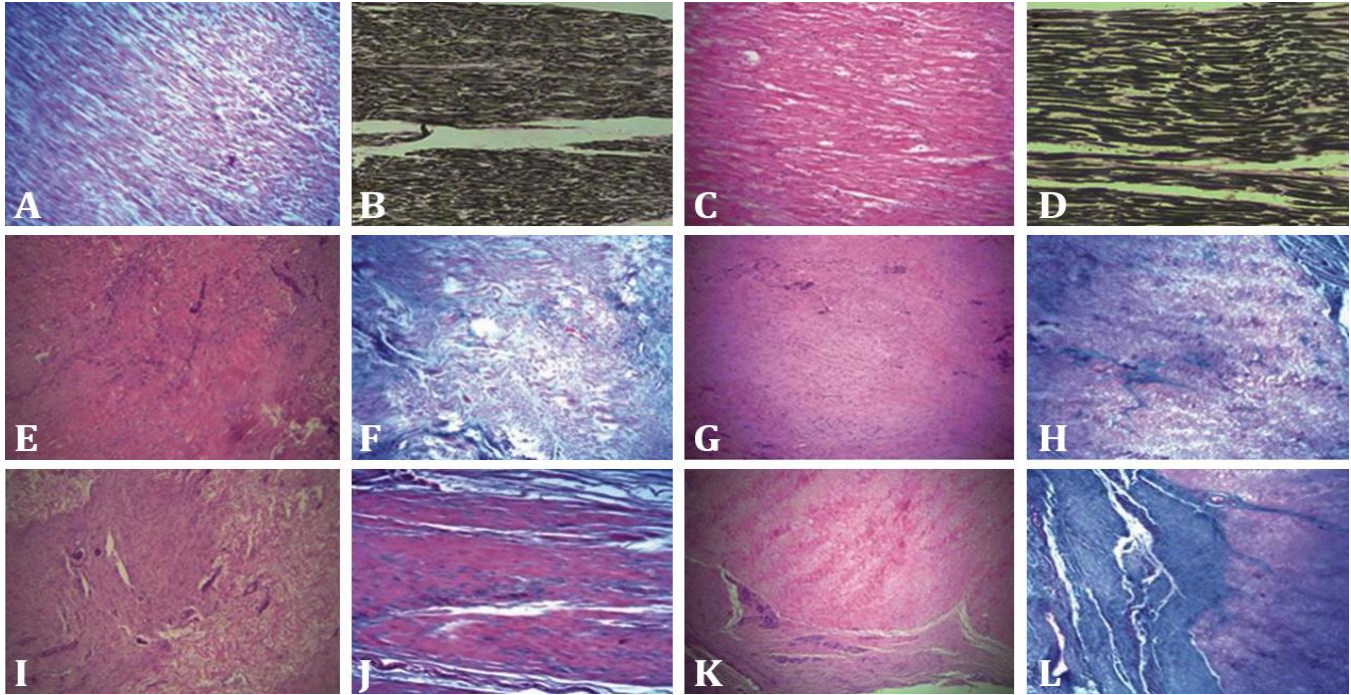


**Fig. 2.** Histopathological characteristics of the transplanted nuchal ligament (NL) autograft and the injured treated tendon on day 120 post-injury. The elastic and collagen fibers are the principal components of the intact, healthy NL in which the elastic fibers are dominant. **A)** In Masson's trichrome (MT) stained sections, the collagen fibers are blue (100 $\times$ ). **B and C)** In Verhoeff's iron Hematoxylin staining, the elastic fibers are black (40 $\times$ , 100 $\times$ ). **D)** In Hematoxylin and Eosin (H&E) staining of NL (200 $\times$ ), the collagen and elastic fibers are matured, crimped, and organized unidirectionally. The tissue is highly cellular with dominant mature fibrocytes that are aligned parallel to collagen fibers. **E and F)** A sample of injured treated tendon belonging to the donkey that died on day 50 shows tendon healing in the proliferative stage. The tissue is highly cellular, mostly irregular, and hypervascular (**E**: H&E, 200 $\times$ ; **F**: MT, 100 $\times$ ). **G and H)** The transplanted tissue is absolutely degraded and replaced with the newly formed tendon. Masson's trichrome staining shows that NL's dominant elastin fibers are replaced with collagen fibers (**G**: H&E, 200 $\times$ ; **H**: MT, 100 $\times$ ). **I and J)** The transplanted tissue is degraded, but its remnants are still observable in the histological section (**I**: H&E, 200 $\times$ ; **J**: MT, 100 $\times$ ). **K and L)** The graft is encapsulated and observed as a part of the primary tissue. No cells are seen in the encapsulated NL (**K**: H&E, 40 $\times$ ; **L**: MT, 40 $\times$ ).

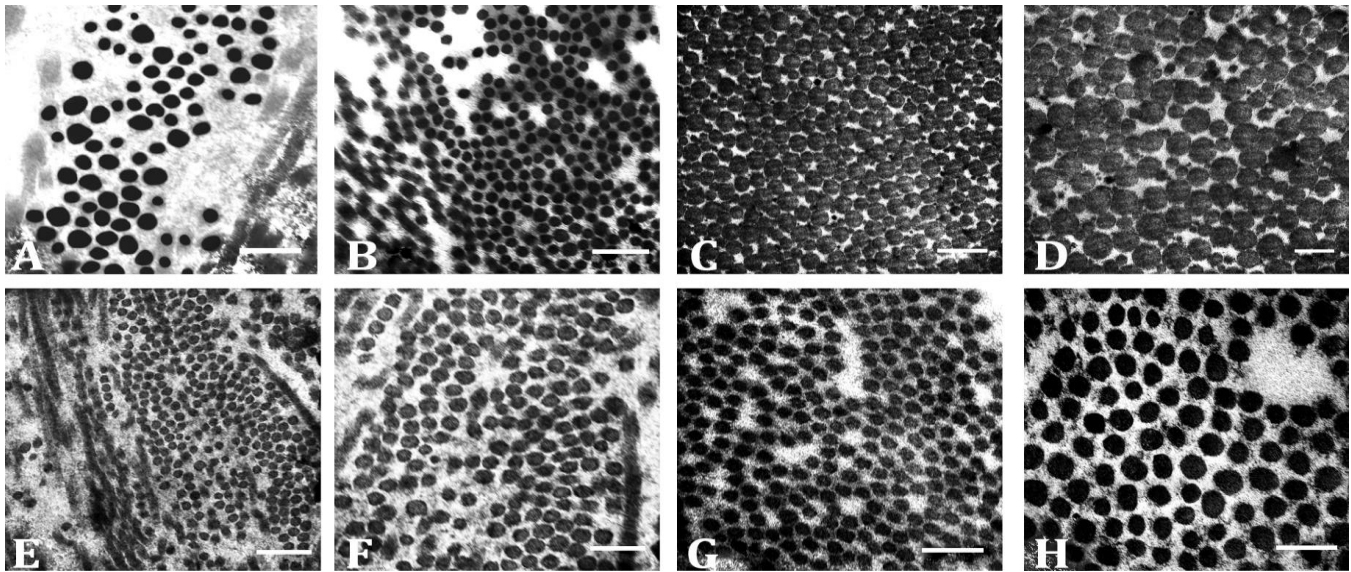


**Fig. 3.** Transmission ultrastructural findings. **A and B)** The nuchal ligament autograft with bimodal collagen fibrils high density of elastic fibers. Central cores of elastic fibers are dense and amorphous (Scale bars in **A**=200 nm; **B**=300 nm). **C and D)** Normal contralateral tendon with a high density of multimodally distributed collagen fibrils (Scale bars in **C**=700 nm; **D**=500 nm). **E and F)** Unimodal distribution pattern of collagen fibrils is seen on 45 post-injury tendons (Scale bar in **E**=400 nm; **F**=200 nm). **G and H)** Injured treated tendon showing numerous newly regenerated collagen fibrils with bimodal distribution (Scale bar in **G**=400 nm; **H**=250 nm).

autograft showed better organization of the collagen fibers than the NL and were completely differentiated into highly aligned collagen bundle and fascicle. However, they still showed a significant difference in their diameter compared to the intact tendon (fiber diameter:  $4.63 \pm 1.15$  vs.  $8.76 \pm 1.79 \mu\text{m}$  (10,000 $\times$ ), collagen bundle diameter:  $51.30 \pm 4.65$  vs.  $63.75 \pm 1.78 \mu\text{m}$  (5,000 $\times$ ), collagen fascicle diameter:  $209 \pm 31.29$  vs.  $227.25 \pm 31.56 \mu\text{m}$  (200 $\times$ ),  $p = 0.01$ ). In the injured treated tendon alike intact tendons, the fascicles could be distinguished easily and were oriented unidirectionally. The organized and properly aligned collagen and elastic fibers of the NL autograft acted as a scaffold for fibroblast migration so that the treated tendons were more cellular even on day 120 postoperatively.

**Transmission electron microscopy.** Treatment significantly amplified the collagen fibrils in the range of 70.00 to 130 and 130 to 250 nm ( $p = 0.001$ ) and significantly enhanced the collagen fibril diameter ( $p = 0.000$ ) and density ( $p = 0.000$ ) compared to the NL. Although the intact tendon's collagen fibrils showed a multimodal distribution pattern. The collagen fibrils of the injured treated tendon were mostly bimodal after four months. They demonstrated lower collagen fibrils' density than the intact tendon after four months of tissue injury (Fig. 3). The sample of injured treated tendon belonging to the donkey that died on day 50 postoperatively showed unimodal distribution pattern in the range of 30.00 to 70.00 nm. There was a significantly lower density of elastic fibers ( $5.71 \pm 2.18$ ) in the injured treated tendon compared to the intact NL specimen ( $60.21 \pm 6.41$ ).

## Discussion

Superficial and deep digital flexor tendons as energy-storing tendons are subjected to relatively high strains during normal physiological activity than positional tendons.<sup>17-19</sup> El-Shafaey *et al.* showed that application of SDFT allograft shielding with glycerol preserved bovine pericardium in experimental superficial digital flexor tendon defect after 90 days was consistent with our results.<sup>8</sup> Dehghani and Varzandian indicated that the bovine fetal tendon xenograft was a good substitute for the case of tendon defect or severe laceration in horses with good biomechanical results without non-weight bearing lameness in a 70-day study.<sup>5</sup>

There is an essential relationship between biomechanical properties and tissue components and how they are located in tissue structure from the molecular level to the visible building.<sup>2,3,7,15,17</sup> In this work, the NL transplant resulted in the restoration of approximately 70.00% and 65.00% of the maximum stress and modulus of elasticity of the healthy intact tendon in the newly regenerated tendon, respectively. The newly regenerated collagen fibrils were highly aligned and were differentiated to larger fibrils, and demonstrated a bimodal pattern.

These resulted in earlier physical activity and enhanced mechanical performance.<sup>20,21</sup> With time and improved differentiation of collagen fibrils, the injured treated tendon's biomechanical properties approximated the intact, healthy tendon.<sup>3,22,23</sup> Increased cross-sectional area and mild to moderate adhesion in the dorsal surface of SDFT were outspread fibrotic tissue that by selecting a suitable size of NL transplant or covering by the artificial sheath, like polydioxanone or glycerol preserved bovine pericardium, the cross-sectional area of repair site may recover and get close to the intact SDFT.<sup>2,7,13</sup>

Ultrasonography of flexor tendon injuries in equidae provides an exact, reliable, safe, and non-invasive method of diagnosis. It accurately reflects the extent of lesions and allows the tendon rehabilitation programs to be tailored by direct visualization of tendon architecture. Ultrasonography of injured tendons demonstrates marked changes in the pattern of their fibers and echogenic intensity depending on the severity of the trauma and structural defects.<sup>13,24</sup> It has been determined that ultrasonographic and histological findings are closely related together during tendon healing.<sup>13,24</sup> It is important to note that the progression in collagen fibers' alignment and enhanced echogenicity in the repair site was correlated with improved physical performance and improved density and maturation collagen fibers in this study.

Blood supply to the tendon is reported to be low, thereby healing is often protracted.<sup>3,22</sup> The NL autograft scaffold stimulated tenoinduction and collagen deposition *in vivo*. Its elastic and collagen components were gradually absorbed or encapsulated and observed as a part of the primary tissue. Therefore, it collaborated at different stages of the healing process so that their components did not degrade quickly, and they had a significant role in aligning the newly regenerated collagen fibrils along their direction. Despite the difference in the ratio of the components of flexor tendons with NL, this autograft was a suitable substrate for the newly regenerated tendon fibers without metaplasia occurring or tissue rejection.

Bimodal distribution of collagen fibril owing to injured treated tendon after 120 days postoperatively indicated improved maturation of tendon tissue compared to the unimodal distribution at an earlier phase of healing, which is in agreement with other studies; however, the morphological and biomechanical parameters were still inferior to the normal tendons yet.<sup>12,16,20,25-27</sup> A relatively similar fiber and cellular structure of the NL to the flexor tendon resulted in the replacement of the NL by a newly formed tendon tissue, or the graft was encapsulated and observed as a part of the primary tissue so that the dominance of collagen fibers replaced the dominance of the elastic fibers. In this work, an experimental tendon defect was created. The authors did not have another option to examine the hypothesis of tendon defect creation. However, sharp and new edges of the tendon

defect created might have improved and hastened the connection of tendon to NL autograft, which could be considered a limitation of the present study.

It seems that the NL is biocompatible, almost biodegradable, and effective in tendon healing. Despite the different structures, NL autograft is a suitable substrate for the newly regenerated tendon fibers without metaplasia or tissue rejection. Further studies in the cases of tendon defect due to any injury should evaluate under NL autograft before suggest the technique for clinicians.

### Acknowledgments

The authors would like to thank the Veterinary Faculty authorities of our universities (Shahid Chamran University of Ahvaz and Shiraz University) for their financial support and kind cooperation.

### Conflict of interest

The authors declare no conflict of interest.

### References

- Bertone AL, Stashak TS, Smith FW, et al. A comparison of repair methods for gap healing in equine flexor tendon. *Vet Surg* 1990; 19(4):254-265.
- Muttini A, Valbonetti L, Abate M, et al. Ovine amniotic epithelial cells: *in vitro* characterization and transplantation into equine superficial digital flexor tendon spontaneous defects. *Res Vet Sci* 2013; 94(1):158-169.
- Avella CS, Smith RKW. Diagnosis and management of tendon and ligament disorders. In: Auer J, Stick J, (Eds). *Equine surgery*. 4<sup>th</sup> ed. USA: Saunders 2012; 1157-1179.
- Moshiri A, Oryan A, Meimandi-Parizi A. Role of tissue-engineered artificial tendon in healing of a large Achilles tendon defect model in rabbits. *J Am Coll Surg* 2013; 217(3):421-441.
- Dehghani S, Varzandian, S. Biomechanical study of repair of tendon gap by bovine fetal tendon transplant in horse. *J Anim V Adv* 2007; 6(9):1097-1100.
- Oryan A, Sharifi P, Moshiri A, et al. The role of three-dimensional pure bovine gelatin scaffolds in tendon healing, modeling, and remodeling: an *in vivo* investigation with potential clinical value. *Connect Tissue Res* 2017; 58(5): 424-437.
- Jann HW, Hart JC, Stein LE, et al. The effects of a cross-linked, modified hyaluronic acid (xCMHA-S) gel on equine tendon healing. *Vet Surg* 2016; 45(2):231-239.
- El-Shafaey El-SA, Karrouf GI, Zaghoul AE. Clinical and biomechanical evaluation of three bioscaffold augmentation devices used for superficial digital flexor tenorrhaphy in donkeys (*Equus asinus*): An experimental study. *J Adv Res* 2013; 4(1):103-113.
- Jahani S, Moslemi HR, Dehghan MM, et al. The effect of butyric acid with autogenous omental graft on healing of experimental Achilles tendon injury in rabbits. *Iran J Vet Res* 2015; 16(1):100-104.
- Chen J, Xu J, Wang A, et al. Scaffolds for tendon and ligament repair: review of the efficacy of commercial products. *Expert Rev Med Devices* 2009; 6(1):61-73.
- Gellman KS, Bertram JEA. The equine nuchal ligament. 1: Structural and material properties. *Vet Comp Orthop Traumatol* 2002; 15(1):1-6.
- Gellman KS, Bertram JEA. The equine nuchal ligament. 2: Passive dynamic energy exchange in locomotion. *Vet Comp Orthop Traumatol Orthop* 2002; 15(1):7-14.
- Parry DA, Craig AS, Barnes GR. Tendon and ligament from the horse: an ultrastructural study of collagen fibrils and elastic fibres as a function of age. *Proc R Soc Lond B Biol Sci* 1978; 203(1152):293-303.
- El-Shafaey El-SA, Karrouf GIA, Zaghoul AEI. A comparative study evaluating three bioscaffold augmentation devices used for superficial digital flexor tenorrhaphy in donkeys (*Equus asinus*) by magnetic resonance imaging and ultrasonography. *J Equine Vet Sci* 2012; 32(11):728-739.
- Butcher MT, Ashley-Ross MA. Fetlock joint kinematics differ with age in Thoroughbred racehorses. *J Biomech* 2002; 35(5):563-571.
- Dowling BA, Dart AJ, Hodgson DR, et al. The effect of recombinant equine growth hormone on the biomechanical properties of healing superficial digital flexor tendons in horses. *Vet Surg* 2002; 31(4):320-324.
- Moshiri A, Oryan A. Structural and functional modulation of early healing of full-thickness superficial digital flexor tendon rupture in rabbits by repeated subcutaneous administration of exogenous human recombinant basic fibroblast growth factor. *J Foot Ankle Surg* 2011; 50(6):654-662.
- Birch HL. Tendon matrix composition and turnover in relation to functional requirements. *Int J Exp Pathol* 2007; 88(4):241-248.
- Dowling BA, Dart AJ, Hodgson DR, et al. Superficial digital flexor tendonitis in the horse. *Equine Vet J* 2000; 32(5):369-378.
- Patterson-Kane JC, Firth EC. The pathobiology of exercise-induced superficial digital flexor tendon injury in Thoroughbred racehorses. *Vet J* 2009; 181(2):79-89.
- Oryan A, Shoushtari AH. Histology and ultrastructure of the developing superficial digital flexor tendon in rabbits. *Anat Histol Embryol* 2008; 37(2):134-140.
- Oryan A, Shoushtari AH. Biomechanical properties and dry weight content of the developing superficial digital flexor tendon in rabbit. *Comp Clin Path* 2009; 18(2):131-137.
- Oryan A, Goodship AE, Silver IA. Response of a collagenase-induced tendon injury to treatment with a polysulphated glycosaminoglycan (Adequan). *Connect*



- Tissue Res 2008; 49(5):351-360.
24. Valdés-Vázquez MA, McCluer JR, Oliver 3<sup>rd</sup> JL, et al. Evaluation of an autologous tendon graft repair method for gap healing of the deep digital flexor tendon in horses. *Vet Surg* 1996; 25(4):342-350.
  25. van Schie HTM, Bakker EM, Cherdchutham W, et al. Monitoring of the repair process of surgically created lesions in equine superficial digital flexor tendons by use of computerized ultrasonography. *Am J Vet Res* 2009; 70(1):37-48.
  26. Oryan A, Moshiri A. A long term study on the role of exogenous human recombinant basic fibroblast growth factor on the superficial digital flexor tendon healing in rabbits. *J Musculoskelet Neuronal Interact* 2011; 11(2): 185-195.
  27. Oryan A, Moshiri A, Meimandi-Parizi AH. Short and long terms healing of the experimentally transverse sectioned tendon in rabbits. *Sports Med Arthrosc Rehabil Ther Technol* 2012; 4(1):14. doi: 10.1186/1758-2555-4-14.